

Short communication

# Physical and electrochemical characterization of Bi<sub>2</sub>O<sub>3</sub>-doped scandia stabilized zirconia

B. Bai<sup>a,\*</sup>, N.M. Sammes<sup>b</sup>, A.L. Smirnova<sup>c</sup>

<sup>a</sup> Department of Mechanical Engineering, University of Connecticut, 44 Weaver Road, Storrs, CT 06269, USA

<sup>b</sup> Department of Metallurgical and Materials Engineering, Colorado School of Mines, CO 80401, USA

<sup>c</sup> Department of Chemical, Materials & Biomolecular Engineering, University of Connecticut, CT 06269, USA

Received 20 September 2007; received in revised form 16 October 2007; accepted 16 October 2007

Available online 30 October 2007

## Abstract

Electrolytes based on Sc<sub>2</sub>O<sub>3</sub>–ZrO<sub>2</sub> exhibit the highest ionic conductivity of zirconia based systems, however, stabilization of the electrochemical properties at operational temperatures, 600–1000 °C, are needed before implementation into SOFCs. Trace additions of Bi<sub>2</sub>O<sub>3</sub> are a known sintering aid for zirconia systems. Crystal structures, electrical properties and long-term stability of Bi<sub>2</sub>O<sub>3</sub>-doped 10ScSZ systems were investigated. The addition of more than 1.0 mol% Bi<sub>2</sub>O<sub>3</sub> resulted in suppression of the rhombohedral to cubic phase transformation at 600 °C and cubic phase stabilization at room temperature. The ionic conductivity of 10ScSZ was also improved by Bi<sub>2</sub>O<sub>3</sub> additions. A maximum conductivity of 0.034 S cm<sup>-1</sup> at 700 °C was observed in 2 mol% Bi<sub>2</sub>O<sub>3</sub>-doped 10ScSZ sintered at 1300 °C. No phase change was observed in 10ScSZ after annealing at 1000 °C. A certain amount of monoclinic phase, and dramatic conductivity decrease, were observed in Bi<sub>2</sub>O<sub>3</sub>-doped samples sintered below 1200 °C after annealing. However, 10ScSZ and 2 mol% Bi<sub>2</sub>O<sub>3</sub>-doped 10ScSZ sintered at 1300 °C show no significant conductivity degradation with annealing. Samples with more than 1 mol% Bi<sub>2</sub>O<sub>3</sub> and sintered above 1300 °C resulted in good ionic conductivity and stability. © 2007 Elsevier B.V. All rights reserved.

**Keywords:** Scandia stabilized zirconia; Bismuth oxide; Electrolyte; IT-SOFC

## 1. Introduction

Scandia stabilized zirconia (ScSZ) has been shown to be an attractive electrolyte material for intermediate temperature solid oxide fuel cells (IT-SOFC), mainly because it exhibits the highest ionic conductivity among all zirconia based oxides [1–4]. The high conductivity of ScSZ is attributed to the small mismatch in size between Zr<sup>4+</sup> and Sc<sup>3+</sup>, leading to a small energy for defect association, which increases mobility of oxygen ions and thus conductivity [5].

The phase equilibrium of the Sc<sub>2</sub>O<sub>3</sub>–ZrO<sub>2</sub> system has been studied by Yamamoto et al. [6,7]. They observed a mixed tetragonal and cubic phase in the system with 5–9 mol% Sc<sub>2</sub>O<sub>3</sub>. Samples with 10–15 mol% Sc<sub>2</sub>O<sub>3</sub> show a rhombohedral phase, which transfers to the cubic phase at approximately 600 °C. The high temperature cubic phase can be stabilized down to

room temperature by adding dopants. Tietz et al. [8] examined Al<sub>2</sub>O<sub>3</sub>-doped ScSZ system and found that although the alumina doping stabilized the cubic zirconia phase down to room temperature, the stabilization was effective only for samples sintered above 1500 °C. Y<sub>2</sub>O<sub>3</sub> additions were also found to improve the phase stability of the ScSZ system [1]. The effect of Bi<sub>2</sub>O<sub>3</sub> on the properties of 10ScSZ have been studied and the addition of 1 and 2 mol% Bi<sub>2</sub>O<sub>3</sub> to 10ScSZ was found to inhibit the cubic–rhombohedral phase transformation and improve the electrical properties [9–11]. The addition of CeO<sub>2</sub> was also observed to stabilize the cubic phase and increase the conductivity of 10ScSZ [12,13].

Despite the high conductivity of the ScSZ system, this electrolyte exhibits unfavourable aging effects [6]. A conductivity of 0.27 S cm<sup>-1</sup> in as-sintered 8ScSZ decreased to 0.13 S cm<sup>-1</sup> after annealing at 1000 °C for 2000 h and no further changes were detected. ScSZ with contents of Sc<sub>2</sub>O<sub>3</sub> up to 11 mol% showed no significant conductivity degradation with annealing [6,7]. The aging effect was attributed to the cubic to tetragonal phase transition [6]. Haering et al. [14] further observed con-

\* Corresponding author. Tel.: +1 860 237 2538; fax: +1 860 486 8378.  
E-mail address: [bai@enr.uconn.edu](mailto:bai@enr.uconn.edu) (B. Bai).

ductivity degradation in aged samples with less than 10 mol%  $\text{Sc}_2\text{O}_3$ . The conductivity of samples with higher scandia content was stable after annealing. A small conductivity decrease in  $\text{Bi}_2\text{O}_3$ -doped 10ScSZ was reported which was thought to be negligible compared to those observed for 8 mol% ScSZ [9].

The present work investigated the crystal structures and electrical properties of ScSZ system with various  $\text{Bi}_2\text{O}_3$  additions by XRD and AC impedance spectroscopy. Long-term phase and electrochemical stabilities were also examined to observe possible aging effects.

## 2. Experimental

10 mol% scandia stabilized zirconia (10ScSZ) was used as the starting material. 10ScSZ powders and  $\text{Bi}_2\text{O}_3$  powders were obtained from Tosoh, Japan and ASARCO, Phoenix, AZ, respectively. Samples were prepared by mixing  $\text{Bi}_2\text{O}_3$  with 10ScSZ in concentrations of 0, 0.5, 1.0 and 2.0 mol%. The powders were mixed with ethanol and ball milled for 68 h. The ball milled powders were cold pressed into pellets under a uniaxial pressure of 200 MPa using a 13 mm floating die. The green bodies were fired at different temperatures from 1000 to 1500 °C for 2 h, with a heating and cooling rate of 3 °C  $\text{min}^{-1}$ .

X-ray diffraction (XRD) was used to examine the crystalline structures of all samples, using a Bruker AXS D5005 diffractometer. The measurements were carried out at room temperature using  $\text{Cu K}\alpha$  radiation. Data was collected in the range of 20–70°  $2\theta$  in the steps of 0.02° at a rate of 5°  $\text{min}^{-1}$ .

Electrical conductivity of the sintered pellets was measured in the temperature range of 300–700 °C using AC impedance spectroscopy. Silver paste was brush painted on both side of the pellets as electrodes and fired at 850 °C for 1 h. The measurements were carried out at 50 °C intervals in air using a Solartron frequency response analyzer (SI 1250) and electrochemical interface (SI 1287) in the frequency range of 0.01 Hz–1 MHz. The AC signal amplitude was varied from 10 to 500 mV. Z-plot software was used to analyze the impedance spectra. XRD and AC impedance measurements were also performed on samples which were subjected to long-term annealing at 700, 800 and 1000 °C.

## 3. Results and discussion

### 3.1. XRD

As shown in Fig. 1, 10ScSZ exhibits a predominantly rhombohedral phase with some percentage of a cubic phase at room temperature. 10ScSZ samples sintered at other temperatures show the similar mixed phase [11]. Powders with 2.0 mol%  $\text{Bi}_2\text{O}_3$  were calcined from 500 to 1500 °C and examined by XRD to study their crystal phases. As shown in Fig. 2, the as-prepared powders show a mixed cubic zirconia and monoclinic  $\text{Bi}_2\text{O}_3$  phase, from 10ScSZ and  $\text{Bi}_2\text{O}_3$ , respectively [13]. The broad peaks suggest a small particle size of the powder. With increasing the calcination temperature, the monoclinic  $\text{Bi}_2\text{O}_3$  phase disappears, suggesting that  $\text{Bi}_2\text{O}_3$  and 10ScSZ are forming a solid solution. The cubic phase peaks were also narrower,

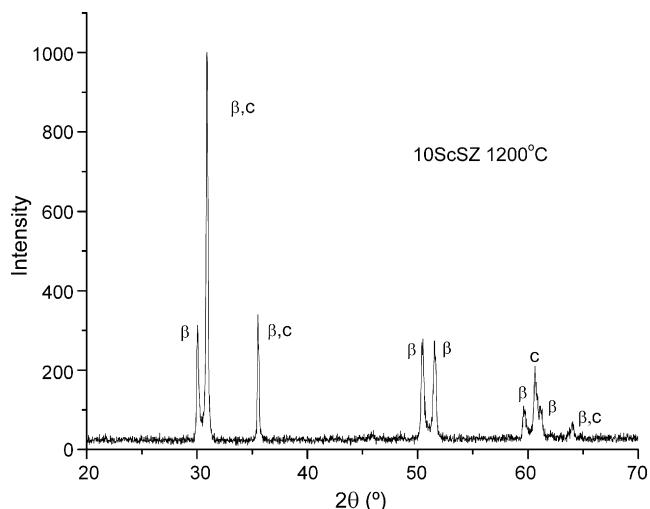


Fig. 1. The XRD pattern of 10ScSZ sintered at 1200 °C (c: cubic;  $\beta$ : rhombohedral).

suggesting the agglomeration of particles and an increase in the particle size. The system shows a sharp cubic phase when calcined at 800 °C suggesting that it has formed a solid solution, as shown in Fig. 2. With further increase in the calcination temperature, the powders start to sinter. The system exhibits a

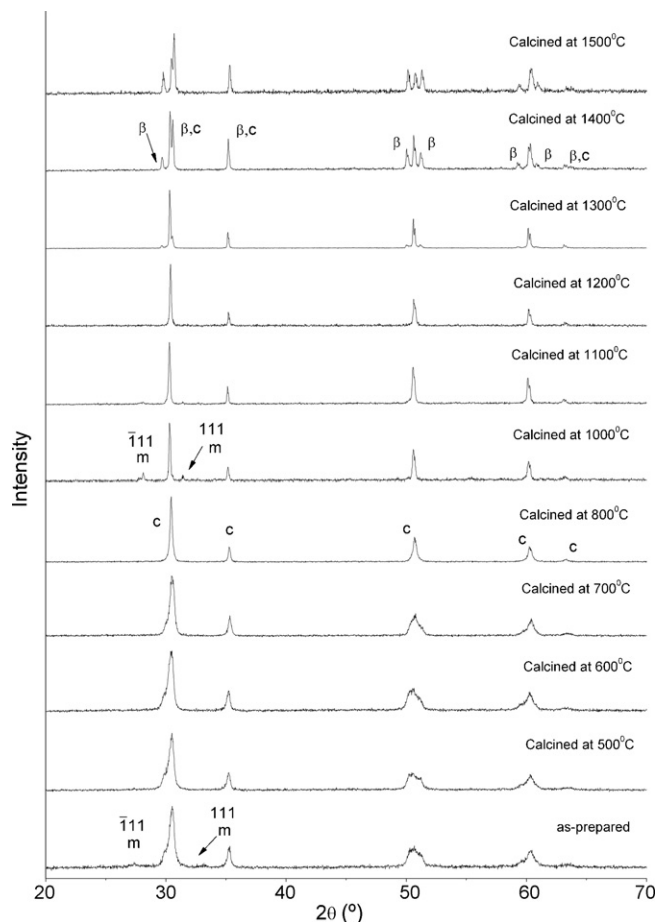


Fig. 2. The XRD patterns of 2 mol%  $\text{Bi}_2\text{O}_3$ -doped 10ScSZ calcined for 2 h at 500–1500 °C (c: cubic;  $\beta$ : rhombohedral; m: monoclinic).

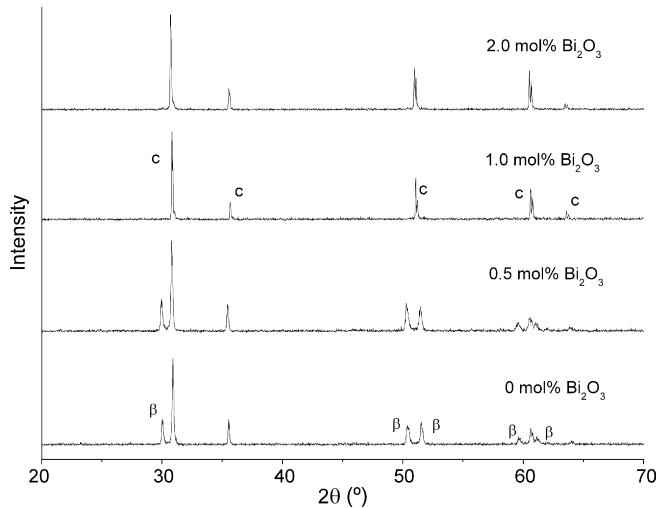


Fig. 3. The XRD patterns of 10ScSZ-doped with 0, 0.5, 1.0 and 2.0 mol%  $\text{Bi}_2\text{O}_3$  sintered for 2 h at  $1300^\circ\text{C}$ .

certain amount of monoclinic zirconia phase when calcined at  $1000$  and  $1100^\circ\text{C}$ . The presence of monoclinic zirconia phase is attributed to the low sintering temperature [9]. A cubic phase was observed in the sample calcined at  $1200^\circ\text{C}$  indicating the addition of  $\text{Bi}_2\text{O}_3$  suppressed the rhombohedral phase in 10ScSZ and fully stabilized the cubic phase to room temperature. A small amount of rhombohedral phase appeared in the sample calcined at  $1300^\circ\text{C}$  and a large amount of rhombohedral phase was observed in the samples calcined at  $1400$  and  $1500^\circ\text{C}$ .  $\text{CeO}_2$ -doped 10ScSZ exhibits a similar mixed rhombohedral and

cubic phase when sintered above  $1300^\circ\text{C}$  [13]. It could possibly be due to the fact that the mixed phase is thermodynamically preferable in the systems sintered at high temperatures. Fig. 3 shows the XRD patterns of the pellet samples with different  $\text{Bi}_2\text{O}_3$  compositions all sintered at  $1300^\circ\text{C}$ . It can be seen that at least 1 mol%  $\text{Bi}_2\text{O}_3$  is needed to maintain the cubic phase [9,11].

### 3.2. Electrical properties

The electrical properties of the sintered pellets were examined using AC impedance spectroscopy. The Nyquist plots have been interpreted with parallel connected RC equivalent circuits where high, intermediate and low frequency semicircles are related to bulk, grain boundary and electrode interface resistances respectively. Fig. 4 shows the impedance spectra for 10ScSZ sintered at  $1200^\circ\text{C}$  and 2 mol%  $\text{Bi}_2\text{O}_3$ -doped 10ScSZ sintered at  $1100^\circ\text{C}$  and measured at different temperatures. The bulk resistance was calculated from the high frequency intercept because it could not be observed at higher temperatures [15]. With increasing temperature, bulk and grain boundary resistances both decrease and the contribution due to grain boundary decreases for both samples. Above  $500^\circ\text{C}$ , the grain boundary resistance disappears, and the electrical conductivity is only attributed to bulk resistance. At lower temperature, i.e.  $300^\circ\text{C}$ , the grain boundary resistance dominates the electrical transport of 10ScSZ. However, with 2.0 mol%  $\text{Bi}_2\text{O}_3$  dopant, the grain boundary resistance was considerably reduced, and thus the electrical properties of the system were significantly improved at lower temperatures.

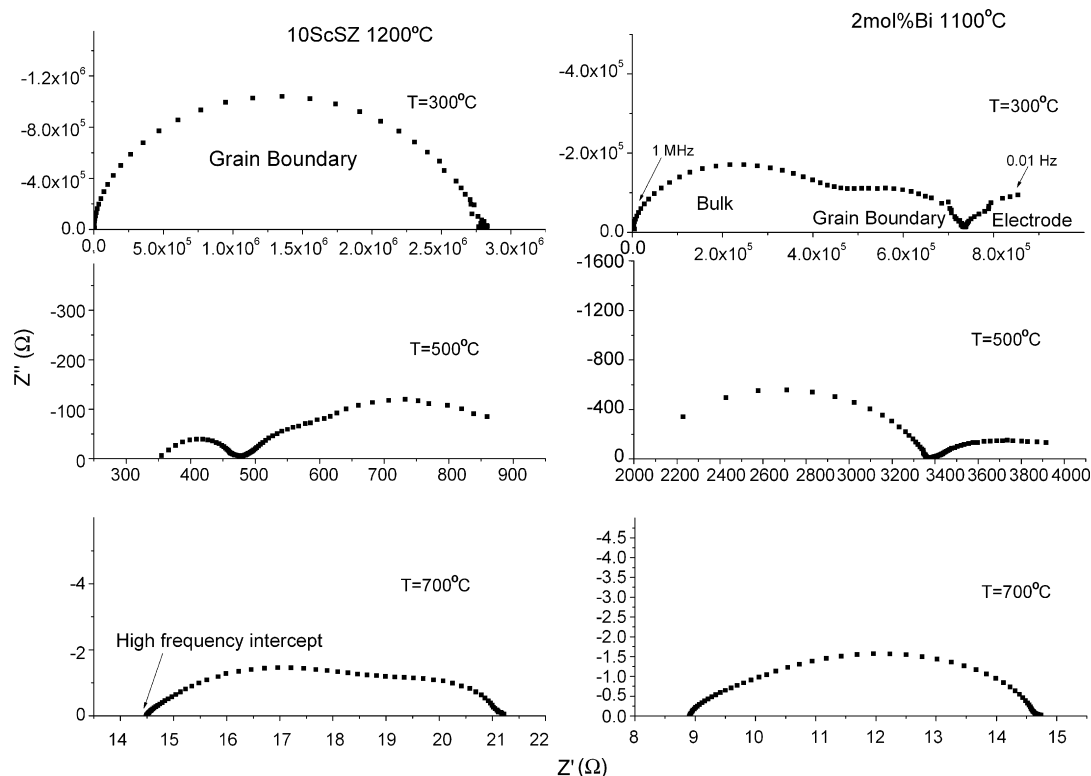


Fig. 4. The impedance spectra of 10ScSZ and 2Bi1100 measured at 300, 500 and  $700^\circ\text{C}$ .

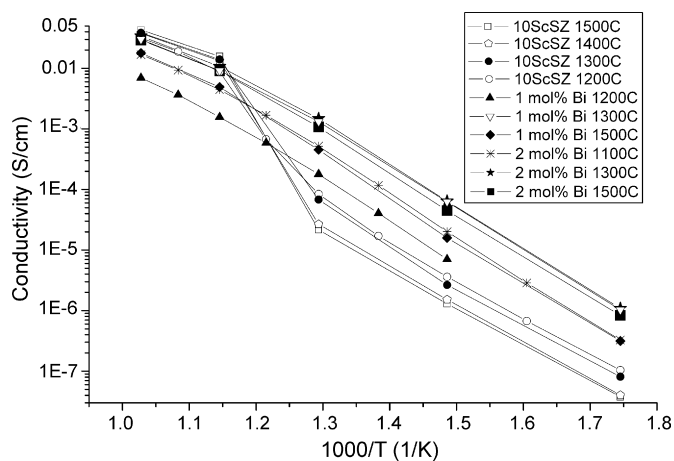


Fig. 5. The temperature dependence of electrical conductivity for 10ScSZ and  $\text{Bi}_2\text{O}_3$  doped pellets sintered at different temperatures.

The temperature dependence of electrical conductivity for the samples is shown in Fig. 5. The total conductivity was calculated by  $\sigma = L/(AR)$ , where  $L$  is the thickness of the pellet;  $A$  is the surface area of the pellet and  $R$  is the total resistance which is determined by the summation of grain boundary resistance and bulk resistance. At measuring temperatures below  $600^\circ\text{C}$ , the  $\text{Bi}_2\text{O}_3$ -doped samples exhibit higher conductivity than 10ScSZ because the grain boundary resistances as well as the total resistances are much lower. However, after the phase transition from rhombohedral to cubic occurs at approximately  $600^\circ\text{C}$  in 10ScSZ, it shows relatively high conductivity which is even higher than the conductivity of 1 mol% and 2.0 mol%  $\text{Bi}_2\text{O}_3$ -doped samples sintered at  $1300^\circ\text{C}$ . This is possibly because 10ScSZ exhibits a cubic phase without being stabilized by a second dopant over  $600^\circ\text{C}$ , and thus has a more open structure and enhanced mobility of charge carriers.  $\text{Bi}_2\text{O}_3$ -doped samples sintered at  $1300^\circ\text{C}$  exhibit higher conductivity than samples sintered at other temperatures, suggesting that  $1300^\circ\text{C}$  is the desired sintering temperature for  $\text{Bi}_2\text{O}_3$ -doped 10ScSZ electrolytes. A maximum conductivity of  $3.42 \times 10^{-2} \text{ S cm}^{-1}$  at

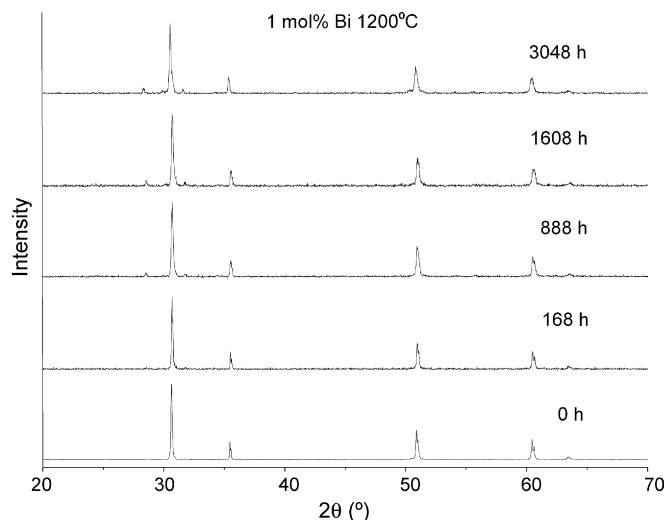


Fig. 7. The XRD patterns of 1Bi1200 after annealing at  $1000^\circ\text{C}$  for 0, 168, 888, 1608 and 3048 h.

$700^\circ\text{C}$  was observed in 2.0 mol%  $\text{Bi}_2\text{O}_3$ -doped 10ScSZ sintered at  $1300^\circ\text{C}$ . Comparable values of conductivity were observed in  $\text{CeO}_2$ -doped 10ScSZ [13].

### 3.3. Long-term stability of the $\text{Bi}_2\text{O}_3$ -doped ScSZ systems

The effect of long-term anneals on the phase and electrical properties of the  $\text{Bi}_2\text{O}_3$ -doped 10ScSZ systems were examined. Samples were annealed at  $1000^\circ\text{C}$  to evaluate the phase transformation by XRD, and at  $700$  and  $800^\circ\text{C}$  to observe the change of electrical properties by ac impedance spectroscopy. Fig. 6 shows the XRD patterns of 10ScSZ sintered at  $1200^\circ\text{C}$  with annealing. No phase change was observed after annealing for 1608 h. The phase present is still a mixture of the dominating rhombohedral and the cubic phase. The XRD patterns of  $\text{Bi}_2\text{O}_3$ -doped sample with annealing are shown in Figs. 7 and 8, respectively. A small amount of monoclinic phase was observed in both of the aged samples with annealing for 3048 h.

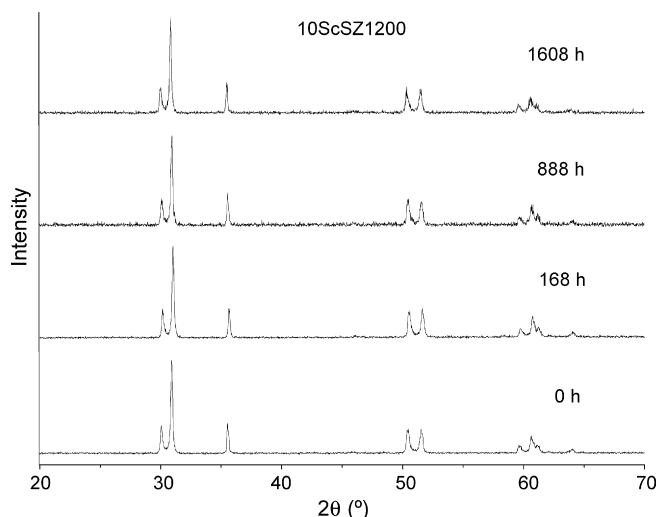


Fig. 6. The XRD patterns of 10ScSZ1200 after annealing at  $1000^\circ\text{C}$  for 0, 168, 888 and 1608 h.

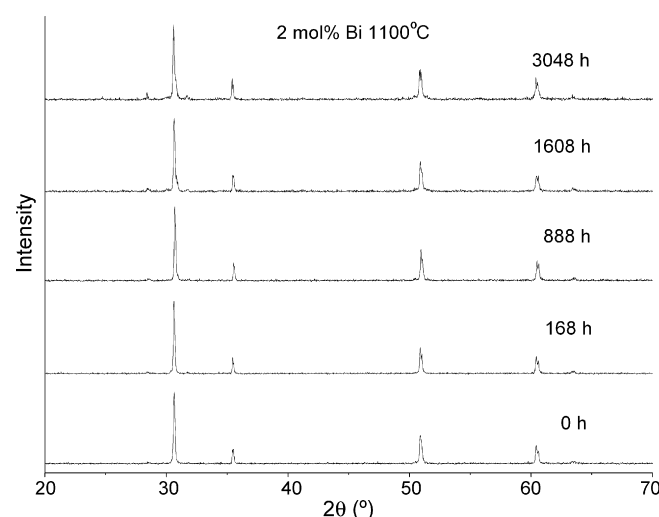


Fig. 8. The XRD patterns of 2Bi1100 after annealing at  $1000^\circ\text{C}$  for 0, 168, 888, 1608 and 3048 h.

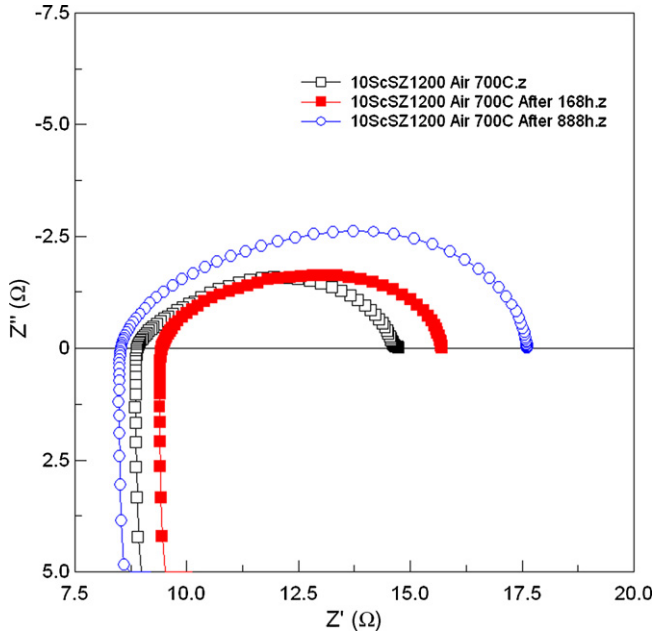


Fig. 9. The impedance spectra of 10ScSZ measured at 700 °C after annealing at 800 °C for 0, 168 and 888 h.

The impedance spectra of the samples with annealing at 800 and 700 °C measured at 700 °C are shown in Figs. 9 and 10, respectively. The high-frequency intercepts in the spectra indicate the total resistance in the electrolyte. As is observed in the figures, the resistance of the two samples changed very little with annealing. In Figs. 11 and 12, the conductivity changes of the four samples at 500 and 700 °C are shown as a function of annealing time. 10ScSZ sintered at 1200 °C shows no significant conductivity degradation. This is in agreement with the literatures that scandia stabilized zirconia containing more

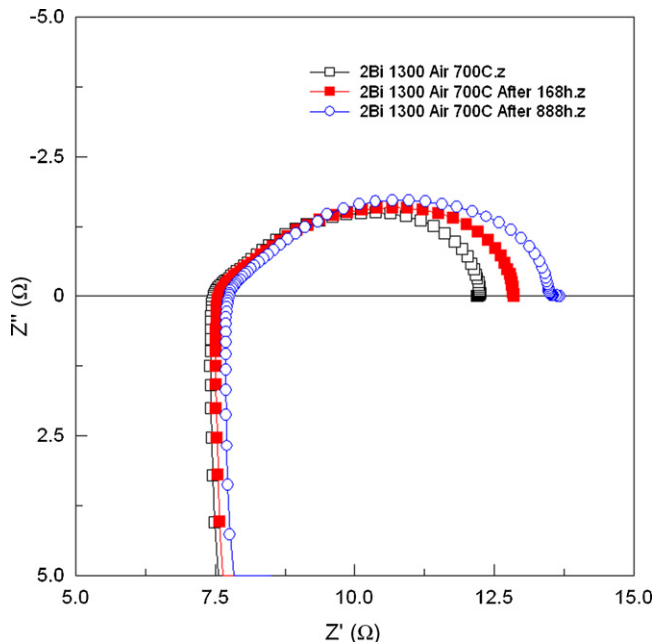


Fig. 10. The impedance spectra of 2Bi1300 measured at 700 °C after annealing at 700 °C for 0, 168 and 888 h.

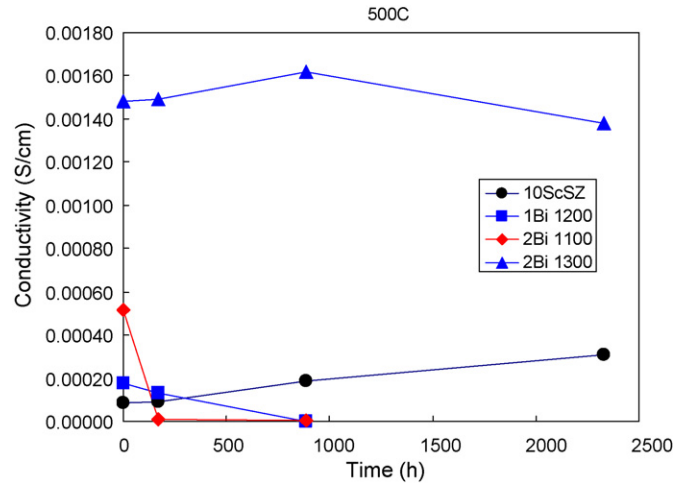


Fig. 11. Conductivity change of 10ScSZ1200, 1Bi1200, 2Bi1100 annealed at 800 °C and 2Bi1300 annealing at 700 °C and measured at 500 °C.

than 10 mol% scandia does not degrade with annealing [6,7,14]. Dramatic conductivity decrease was observed in 1 mol% Bi<sub>2</sub>O<sub>3</sub>-doped 10ScSZ sintered at 1200 °C (1Bi1200) and 2 mol% Bi<sub>2</sub>O<sub>3</sub>-doped 10ScSZ sintered at 1100 °C (2Bi1100) after annealing at 800 °C for 888 h. At 700 °C, the conductivity decreased from  $6.95 \times 10^{-3} \text{ S cm}^{-1}$  to  $4.24 \times 10^{-5} \text{ S cm}^{-1}$  in 1Bi1200, and from  $1.68 \times 10^{-2} \text{ S cm}^{-1}$  to  $1.38 \times 10^{-4} \text{ S cm}^{-1}$  in 2Bi1100. The result for 1Bi1200 is in disagreement with the result shown in [9]. However, 2.0 mol% Bi<sub>2</sub>O<sub>3</sub>-doped 10ScSZ sintered at 1300 °C (2Bi1300) shows only little degradation with annealing at 700 °C. The reasons for the degradation in 1Bi1200 and 2Bi1100 could potentially be very complicated. The annealing temperature of 800 °C is not a concern because large conductivity degradation was also observed when 2Bi1100 was annealed at 700 °C as shown in Fig. 13. The presence of monoclinic phase in these samples could be postulated as the reason for this anomaly [11].

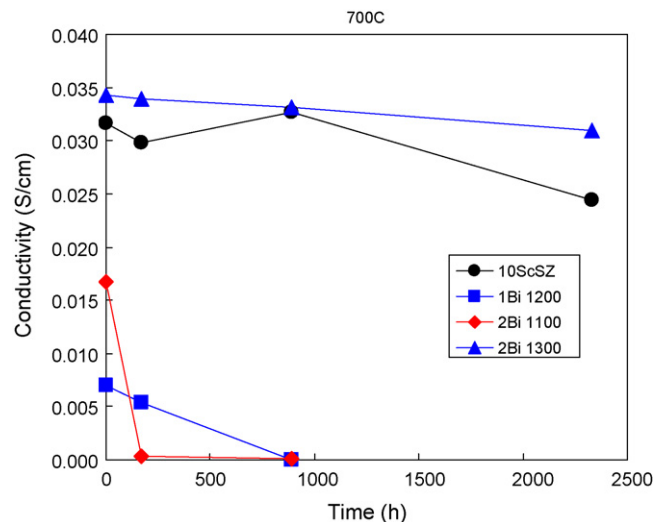


Fig. 12. Conductivity change of 10ScSZ1200, 1Bi1200, 2Bi1100 annealed at 800 °C and 2Bi1300 annealing at 700 °C and measured at 700 °C.

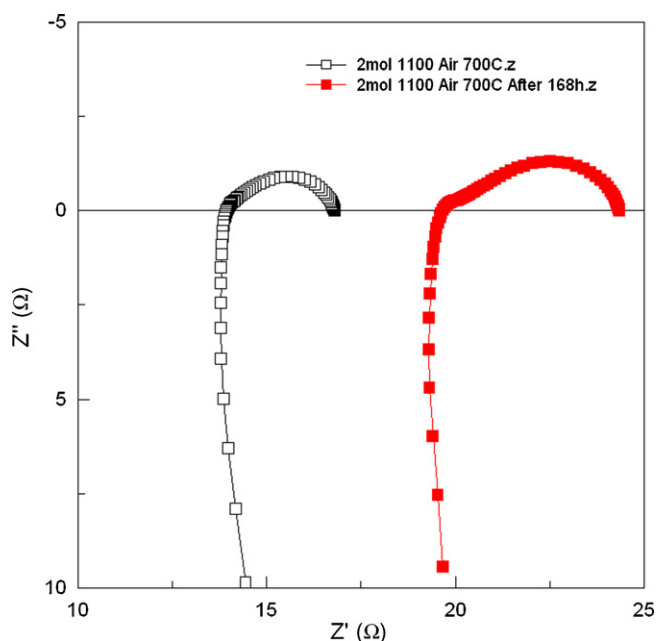


Fig. 13. The impedance spectra of 2Bi1100 measured at 700 °C after annealing at 700 °C.

#### 4. Summary

The addition of  $\text{Bi}_2\text{O}_3$  aided the sintering process in 10ScSZ and allowed the samples to sinter at lower temperature. By adding more than 1.0 mol%  $\text{Bi}_2\text{O}_3$  to 10ScSZ, the cubic–rhombohedral phase transformation at 600 °C in 10ScSZ was eliminated and the cubic phase was stabilized to room temperature. The electrical conductivity of 10ScSZ was also improved by adding  $\text{Bi}_2\text{O}_3$ . A maximum conductivity of  $3.42 \times 10^{-2} \text{ S cm}^{-1}$  at 700 °C was observed in 2Bi1300. No phase change was observed in 10ScSZ after annealing at 1000 °C for 1608 h. A certain percentage of a monoclinic phase was observed in 1Bi1200 and 2Bi1100 after annealing for 3048 h. Dramatic conductivity decrease was observed in 1Bi1200 and 2Bi1100 after annealing at 800 °C for 888 h. However, 10ScSZ

and 2Bi1300 show no significant conductivity degradation with annealing. Samples with more than 1 mol%  $\text{Bi}_2\text{O}_3$  and sintered above 1300 °C have a good combination of electrical conductivity and stability.

#### Acknowledgements

This work was financially supported by Connecticut Innovations Inc., Contract No. 05Y07 and New Energy and Industrial Technology Development Organization (NEDO) Advanced Ceramic Reactor Project, Contract No. AG060145.

#### References

- [1] T.I. Politova, J.T.S. Irvine, *Solid State Ionics* 168 (2004) 153–165.
- [2] S.P.S. Badwal, F.T. Ciacchi, D. Milosevic, *Solid State Ionics* 136/137 (2000) 91–99.
- [3] Z. Lei, Q. Zhu, *Solid State Ionics* 176 (2005) 2791–2797.
- [4] O. Yamamoto, *Electrochim. Acta* 45 (2000) 2423–2435.
- [5] J.W. Fergus, *J. Power Sources* 162 (2006) 30–40.
- [6] O. Yamamoto, Y. Takeda, N. Imanishi, Y. Arati, H. Sakai, Y. Mizutani, M. Kawai, Y. Nakamura, N. Sammes, *Solid State Ionics: New Dev.* (1996) 221–233.
- [7] O. Yamamoto, Y. Arati, Y. Takeda, N. Imanishi, Y. Mizutani, M. Kawai, Y. Nakamura, *Solid State Ionics* 79 (1995) 137–142.
- [8] F. Tietz, W. Fischer, Th. Hauber, G. Mariotto, *Solid State Ionics* 100 (1997) 289–295.
- [9] M. Hirano, T. Oda, K. Ukai, Y. Mizutani, *Solid State Ionics* 158 (2003) 215–223.
- [10] S. Sarat, N.M. Sammes, A. Smirnova, *J. Power Sources* 160 (2006) 892–896.
- [11] B. Bai, N.M. Sammes, A. Smirnova, G. Tompsett, *Proceedings of the 4th International Conference on Fuel Cell Science, Engineering and Technology*, Irvine, CA, June 19–21, 2006, 2006.
- [12] Z. Wang, M. Cheng, Z. Bi, Y. Dong, H. Zhang, J. Zhang, Z. Feng, C. Li, *Mater. Lett.* 59 (2005) 2579–2582.
- [13] B. Bai, W.A.G. McPhee, A.L. Smirnova, N.M. Sammes, *ECS Transactions*, vol. 7, Nara, Japan, 2007.
- [14] C. Haering, A. Roosen, H. Schichl, M. Schnoller, *Solid State Ionics* 176 (2005) 261–268.
- [15] I. Kosacki, H.U. Anderson, Y. Mizutani, K. Ukai, *Solid State Ionics* 152/153 (2002) 431–438.